Journal of Affective Disorders 405 (2026) 121550

Contents lists available at ScienceDirect

Journal of Affective Disorders

journal homepage: www.elsevier.com/locate/jad

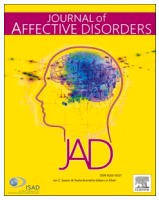

Research paper

Shift to the core: Abnormal core-periphery global topography in unipolar and bipolar depression

Andrea Scalabrini [a,e,*], Mariagrazia Palladini [b], Sara Poletti [b,c], Benedetta Vai [b,c], Federico Calesella [b], Marco Paolini [b], Giulia Gulino [b], Sara Masoumi [e], Raffaella Zanardi [d], Cristina Colombo [c,d], Georg Northoff [e], Francesco Benedetti [b,c]

[a] University of Bergamo, Department of Human and Social Sciences, Bergamo, Italy
[b] Psychiatry & Clinical Psychobiology, Division of Neuroscience, IRCCS Ospedale San Raffaele, Milan, Italy
[c] University Vita-Salute San Raffaele, Milan, Italy
[d] Mood Disorders Unit, IRCCS Ospedale San Raffaele, Milano, Italy
[e] The Royal's Institute of Mental Health Research, University of Ottawa Institute of Mental Health Research, Ottawa, Canada

A B S T R A C T

This study explores the global signal topography of core and periphery brain networks in Major Depressive Disorder (MDD), Bipolar disorder (BD-Dep) and healthy controls (HC) using resting-state fMRI. In a sample of 140 depressed MDD and BD patients, and 70 HC, we observed a significant shift toward increased activity in the transmodal-core regions (e.g., default mode network, frontoparietal network) at the expense of unimodal-periphery regions (e.g., visual, sensory-motor cortices) in both depressed MDD and BD patients compared to HC. Whole brain machine learning analyses further demonstrated that altered global signal dynamics can effectively distinguish MDD and BD from HC (ACC = 79% and 77% respectively). Notably, we identified a significant negative correlation between global signal correlation in unimodal-periphery networks and depressive symptom severity. Additionally, in a smaller sample of BD during mania ($N = 22$) a distinct topographic pattern was observed, with increased global representation in the unimodal-periphery compared to depressive states, suggesting mood state-dependent shifts in network organization. To assess multivariate discriminability across diagnostic groups, a Partial Least Squares (PLS) analysis revealed that higher Core and related network activity (DMN, FPN) predicted diagnostic assignment to MDD and BD-Dep, whereas higher Periphery and related network (e.g., visual and sensory-motor networks) predicted assignment to BD-Man and HC. The Core–Periphery (C–P) ratio emerged as the strongest predictor (VIP = 1.65). These results underscore the critical role of global signal topography in mood disorders, particularly the imbalance between core and peripheral brain networks, as a potential neurobiological marker for depressive states.

1. Introduction

Depression represents a major global contributor to lifelong disability, imposing both economic and societal burdens (Wittchen, 2012). Major depressive episodes may occur in Major Depressive Disorder (MDD) and in Bipolar Disorder (BD), where depressive phases alternate with hypomanic or manic episodes (Cuellar et al., 2005). Resting-state functional MRI (rs-fMRI) has become a central tool for investigating the neurobiological mechanisms underlying these conditions, consistently revealing abnormalities in large-scale intrinsic brain networks such as the Default Mode Network (DMN), Frontoparietal Network (FPN), and Salience Network (SN) (Davey et al., 2016; Berger, 1929; Northoff, 2016a; Raichle, 2015; Raichle et al., 2001). Altered resting state dynamics within these networks, particularly in the DMN and FPN have been repeatedly associated with symptoms such as rumination, excessive mind-wandering, and heightened self-focus (Price and Drevets, 2010; Buckner et al., 2008). Additionally, changes have been observed in unimodal sensory and motor regions, further suggesting a global imbalance of brain activity (Liu et al., 2022; Martino et al., 2020; Martino et al., 2016; Northoff et al., 2018; Quraishi and Frangou, 2002; Scalabrini et al., 2025a; Song et al., 2021; Song et al., 2024a). This perspective aligns with the notion that large-scale brain organization is shaped by a core–periphery (C–P) architecture, whereby integrative transmodal "core" regions (e.g., DMN, FPN) are distinguished from sensory–motor "periphery" regions, suggesting that an imbalance in this C–P topography may characterize mood disorders (Doucet et al., 2020; Hamilton et al., 2012; Hamilton et al., 2011; Janiri and Frangou, 2022; Northoff and Hirjak, 2024; Zhou et al., 2010). However, this topographic imbalance has yet to be empirically investigated by comparing the depressive episodes in the two disorders, which

* Corresponding author at: Departmento of Human and Social Sciences, University of Bergamo, P.le S. Agostino, 2, Bergamo, 24129, Italy.
E-mail address: andrea.scalabrini@unibg.it (A. Scalabrini).

https://doi.org/10.1016/j.jad.2026.121550
Received 16 December 2025; Received in revised form 8 February 2026; Accepted 28 February 2026
Available online 3 March 2026

is the main aim of the present study.

Increased connectivity within the DMN, particularly between regions such as the medial prefrontal cortex and hippocampus, has been consistently reported in MDD (Hao et al., 2020; Kaiser et al., 2015; Zhang et al., 2018). More recent work has shifted attention toward global signal dynamics, particularly global signal correlation (GSCORR) (Ao et al., 2021; Liu et al., 2017; Murphy and Fox, 2017; Yang et al., 2024), which examines the spatial average of the time-varying BOLD signal across the entire brain (Scalabrini et al., 2020). Abnormal GSCORR patterns have been observed in DMN hubs during both rest and task states and have been linked to depressive symptoms (Abdallah et al., 2017; Murrough et al., 2016; Scheinost et al., 2018) as well as to treatment responses (Yang et al., 2024). Scalabrini et al. (Scalabrini et al., 2020) further showed that alterations in both within-DMN and DMN–non-DMN connectivity result in a reorganization of global signal topography in MDD, characterized by a shift toward greater global representation of DMN regions. This shift reflects a bias toward internally oriented cognition, consistent with symptoms such as rumination and heightened self-referential processing (Northoff, 2007; Northoff, 2016b; Northoff, 2024). In addition, recent findings emphasize the contribution of unimodal periphery regions, with reduced activity in visual cortex correlating with overall depressive severity and psychomotor retardation (Liu et al., 2022; Scalabrini et al., 2025b; Song et al., 2024b).

Literature on global signal dynamics in BD is limited, but available evidence indicates mood-state–dependent shifts in global signal topography. Zhang et al. (Zhang et al., 2019) reported that during manic episodes, BD patients show increased global signal in motor regions, consistent with heightened psychomotor activity and agitation. In contrast, BD depression is characterized by increased global signal in the hippocampus, potentially reflecting enhanced autobiographical memory processing. These findings suggest that alterations in global signal topography also characterize BD and vary systematically across mood states.

Mood disorders, particularly during depressive episodes, are thought to involve a dysfunctional shift from unimodal sensory regions toward transmodal core networks, accompanied by altered global signal dynamics (Liu et al., 2022; Scalabrini et al., 2020; Lu et al., 2022). Such imbalance may contribute to key depressive symptoms, including excessive self-focus, rumination, and disruptions in internally directed cognition. Despite growing evidence, the precise nature of this core–periphery alteration in MDD and BD—especially during depressive episodes—remains insufficiently understood.

1.1. Aims of the study

The primary aim of this study is to examine differences in global core–periphery topography across individuals with MDD, BD during depressive episodes (BD-Dep), and healthy controls (HC), focusing on the balance between transmodal-core and unimodal-periphery networks. We assessed both voxel-wise and network-level global signal dynamics and examined whether these alterations relate to depressive symptom severity. As a preliminary proof of concept, we also explored global signal patterns in BD mania (BD-Mania) to identify potential state-dependent shifts in core–periphery organization.

Drawing on prior findings (Scalabrini et al., 2020; Lu et al., 2022; Zhang and Northoff, 2022), we hypothesized that both MDD and BD-Dep would show a common shift toward increased global representation of core transmodal networks (e.g., DMN, FPN) and reduced representation of unimodal sensory–motor regions. We further expected these alterations to emerge in both voxel-wise and network-of-interest analyses, to correlate with depressive symptom severity, and to support diagnostic classification of MDD and BD-Dep relative to HC using machine-learning approaches. Finally, we hypothesized that BD-Mania would show a distinct, state-dependent shift, characterized by relatively greater activity in unimodal periphery networks.

1.2. Experimental procedures

The sample included 140 inpatients with a major depressive episode, either with a diagnosis of MDD ($n = 70$) or BD (n = 70) and 22 inpatients with a manic episode of illness, consecutively admitted at the Mood Disorder Unit of IRCCS Ospedale San Raffaele in Milan, Italy. Seventy healthy participants served as controls.

Descriptive statistics and differences between groups are reported in Table 1.

Clinical assessment, fMRI data acquisition, and preprocessing are reported in Supplementary materials.

After a complete description of the study, written informed consent was obtained. All research activities were approved by the local ethical committee.

1.3. fMRI analyses

The fMRI analysis followed a four-step approach. First, voxel-wise GSCORR maps were used to compare whole-brain topography in depressive episodes (MDD, BD-Dep) versus healthy controls. Second, a network-of-interest analysis examined Core (DMN, FPN, Limbic) and Periphery (Visual, SMN, DAN, VAN) networks across groups, supplemented by machine learning to test the predictive value of these features

Table 1
Descriptive statistics.

	HC (n = 70)	MDD (n = 70)	BD-Dep (n = 70)	BD-Man (n = 22)	p	Post-hoc
Age	28.34 ± 7.70	51.65 ± 10.00	47.69 ± 13.01	44.95 ± 11.50	<0.001	HC < MDD, BD-Dep, BD-Man
Sex (F/M)	37/33	35/35	34/36	14/9	0.679	
Education (yrs)	16.03 ± 3.08	12.87 ± 3.92	12.26 ± 3.67	12.65 ± 4.98	<0.001	HC > MDD, BD-Dep, BD-Man
Duration of illness (yrs)	–	16.57 ± 12.54	19.00 ± 12.12	12.00 ± 10.16	0.053	
BDI score	–	14.50 ± 8.12	14.23 ± 8.94	–	0.389	
Imipramine eq.	–	173.14 ± 78.73	131.49 ± 100.04	2.61 ± 12.51	<0.001	MDD > BD-Dep, BD-Man BD-Dep > BD-Man
Chlorpromazine eq.	–	16.1 ± 41.9	8.51 ± 23.1	208 ± 167	<0.001	MDD > BD-Dep, BD-Man BD-Dep > BD-Man
Lorazepam eq.	–	0.53 ± 1.04	2.06 ± 7.80	1.93 ± 2.41	0.201	
Lithium (N/Y)	–	67/3	36/34	7/16	<0.001	MDD < BD-Dep, BD-Man

and by correlations with depressive symptoms. Third, to assess the specificity of Core–Periphery disruptions to depressive states, we included a smaller sample of BD individuals scanned during mania (BD-Man, $N = 22$), acknowledging the practical challenges and reduced statistical power inherent in scanning manic patients. Finally, Partial Least Squares (PLS) analysis was conducted to evaluate the multivariate discriminability of whole-brain GSCORR patterns across all diagnostic groups.

2. Voxelwise analysis

2.1. Calculation of global brain activity—GSCORR

As a first step GSCORR was calculated as the Pearson correlation between the GS and all the other voxels in the whole brain gray matter with Fisher z transformation (Power et al., 2012). Group comparisons were performed using AFNI's function "3dANOVA". The results were thresholded at $p < 0.001$ (FDR corrected; with a minimum cluster size of 40 voxels) (See Fig. 1). Statistical maps were thresholded at $p = 0.001$, False Discovery Rate-corrected (FDR-p) of $p < 0.05$ with a minimum cluster size of 100 significant voxels (Zhu et al., 2019).

Statistical maps (Fig. 1) were thresholded at a voxel-wise threshold of $p < 0.001$ and corrected for multiple comparisons using false discovery rate (FDR) at $q < 0.05$, with a minimum cluster extent of 100 contiguous voxels (Zhu et al., 2019). Global signal regression was not applied, as the primary outcome (GSCORR) quantifies voxelwise coupling with the global signal. Applying GSR removes the defining signal component and can induce sign inversions by construction; a GSR-based sensitivity analysis is therefore reported in the Supplementary Material (Fig. S1). Sensitivity analyses on pharmacological exposure indicated that medication load did not account for the observed Core–Periphery topographic organization, nor for its association with

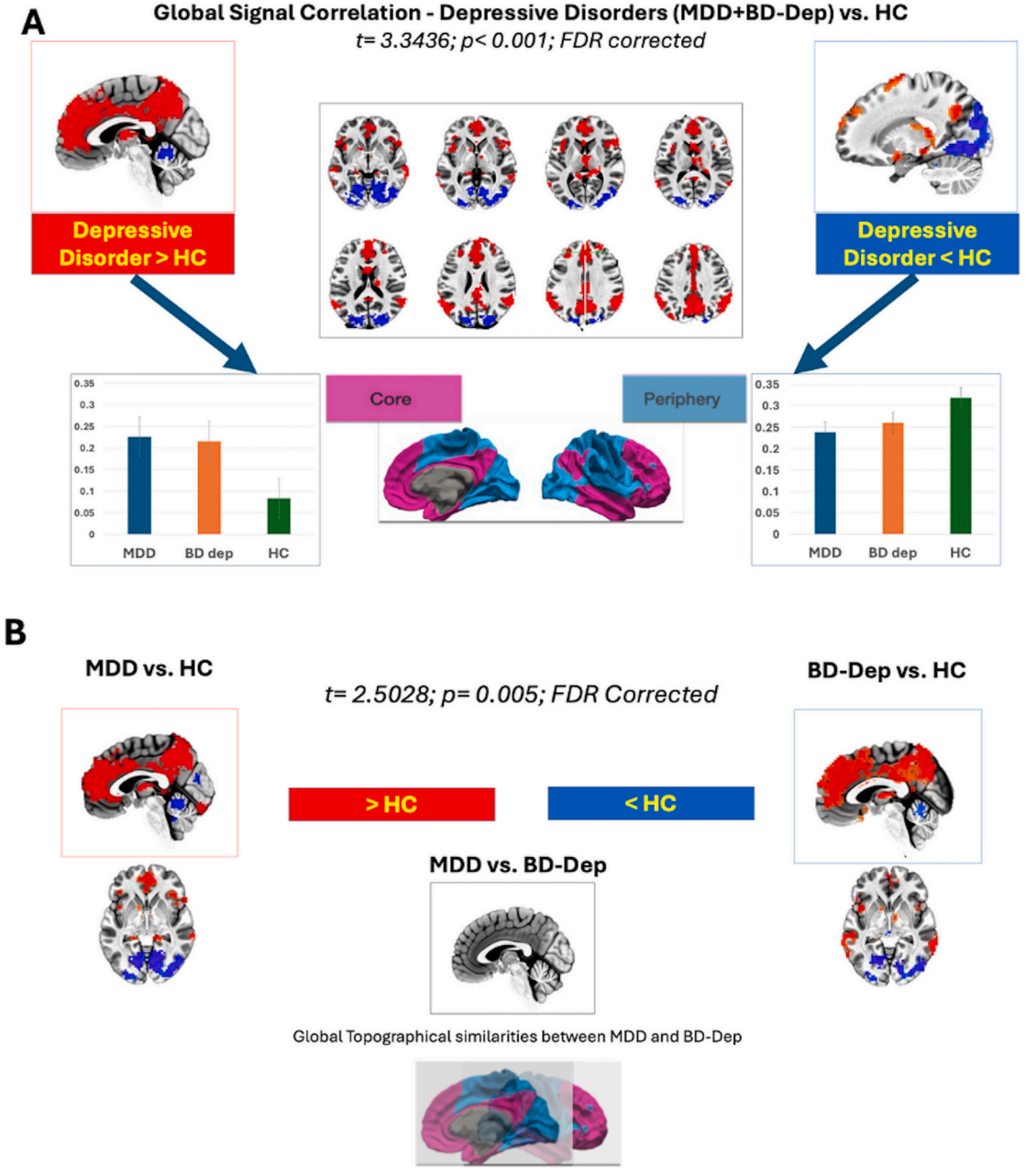

Fig. 1. Global brain topography. A) Whole brain global signal correlation (GSCORR) topography of depressive disorders, i.e., Major Depressive Disorder and Bipolar Disorder in Depressive state (MDD + BD-Dep) vs. Healthy Controls (HC). B) Independent comparisons: MDD vs. HC; BD-Dep vs. HC and MDD vs. BD-Dep.

depressive symptom severity (see Supplementary Materials).

2.2. Individual classification of subjects—machine learning using support vector machine

To assess whether global signal topography discriminates diagnostic groups, we performed multivariate pattern classification on GSCORR maps using support vector machines (SVM) implemented in PRoNTo 2.1. (http://www.mlnl.cs.ucl.ac.uk/pronto). Binary classifications included MDD vs. HC, BD vs. HC, and MDD vs. BD. Model performance was evaluated using stratified 5-fold nested cross-validation with hyperparameter optimization (Baars, 2005; Dehaene et al., 2011; Mashour et al., 2020) and to assess model's performance. Nested cross-validation scheme has been shown to provide more reliable estimates than other validation procedures such as leave one-out (Varoquaux, 2018).

Predictions obtained in the test set allow defining balanced accuracy (BA) value, computed as the average of the class accuracies (corresponding to the sensitivity for mood disorders and specificity for HC), positive (PPV) and negative predictive values (NPV) and area under the receiver operator curve (AUC). We also estimated the statistical significance ($p < 0.05$) of accuracies by using 5000 permutations of the labels during training phase.

Voxel-wise SVM weight maps were computed for visualization purposes and are reported in the Supplementary Material (Fig. S2). These maps represent multivariate discriminative patterns rather than independent voxel-wise effects (Schrouff et al., 2013).

3. Network of interest approach

3.1. Core-periphery similarities and differences between groups

GSCORR values were extracted from predefined large-scale functional networks following established parcellation frameworks (Yeo et al., 2011a) Networks were grouped into Core (DMN, FPN, Limbic) and Periphery (Visual, Somatomotor, Dorsal Attention, Ventral Attention). A Core–Periphery (C–P) ratio was computed to quantify the balance between transmodal and unimodal systems.

To assess group differences in large-scale topography, we performed a 2 (Topography: Core vs. Periphery) × 3 (Group: MDD, BD-Dep, HC) ANCOVA including age, sex and education as covariates. We then examined each of the seven canonical networks individually to identify which networks contributed to the observed core–periphery effects. Moreover, to test for diagnostic predictivity we performed a series of ROC (Receiver Operating Characteristic) curves on Core, Periphery and on the ratio between the two, i.e., Core-Periphery (C–P ratio) (see Supplementary material, Fig. S3).

We then examined each of the seven canonical networks individually to identify which networks contributed to the observed core–periphery effects. As a sensitivity check, we repeated the analyses in an age-matched subsample (patients vs. controls), obtaining a highly similar pattern of group differences in GSCORR (see Supplementary Materials for full details, Table S2).

3.2. GSCORR-depressive symptoms correlation

Associations between GSCORR values and depressive symptom severity were examined using Pearson correlations between Core and Periphery network GSCORR (Yeo et al., 2011a) and BDI scores. Partial correlations controlling for age, sex and education were computed. To assess the robustness of these associations against potential pharmacological confounds, additional sensitivity analyses controlling for medication load were conducted and are reported in the Supplementary Materials (Table S4).

3.3. Testing the difference between depressive vs. manic dimension - introduction of bipolar disorder in manic state

To evaluate whether core–periphery alterations vary across mood states, we included 22 BD patients scanned during a manic episode (BD-Man). This proof-of-concept step tested whether global signal topography differs between manic and depressive states. A chained ANCOVA approach was applied: first assessing Core–Periphery balance across groups (HC, MDD, BD-Dep, BD-Man), followed by network-level analyses. Including BD-Man enabled examination of a potential continuum from healthy controls to depressive and manic states. This approach provided a more nuanced understanding of the psychopathological spectrum in mood disorders.

3.4. Individual classification of subjects—machine learning using PLS

Given the above, we wondered whether Core-Periphery imbalances as proxied by GSCORR may potentially serve as a reliable biomarker for distinguishing mood states.

To this end, we performed a partial least square (PLS) regression entering GSCORR values for Core, Periphery, Core/Periphery ratio, together with metrics for each network separately as independent variables predicting mood state category (BD-manic, BD-dep, MDD, HC). PLS allows creating composite variables of X data, but unlike PCA, it exploits information in the dependent variable to rank the composite variables and order them by their correlations with the response in the regression model. The accuracy of the predictive value of the model was assessed by using the Nonlinear Iterative Partial Least Squares (NIPALS) algorithm (Akarachantachote et al., 2014; Palermo et al., 2009; Wold, 1966) and optimizing by cross-validation the number of PLS components to extract (A), then calculating R2X (a A-dimensional vector, to record the explained variance of the data matrix of predictors by each PLS component), R2Y (a A-dimensional vector, to record the explained variance of response variables by each PLS component); and for each variable predictive weights (w), and the variable importance in projection (VIP) values, to estimate the contribute of each variable to the explanation of the Y variance and the direction of effect. The significance of variables contributions was defined by VIP >1 (Akarachantachote et al., 2014; Palermo et al., 2009; Bravi et al., 2025).

4. Results

4.1. Neural global signal topography in depression

4.1.1. Abnormal voxel-wise global topography in depressed MDD and BD vs Healthy controls

Voxel-wise ANOVA on GSCORR maps revealed a significant group effect ($F = 5.63$, $p = 0.001$, FDR-corrected) in a large cluster primarily involving core DMN regions (Fig. 1; Table S1). Post hoc comparisons showed that both depressive groups combined (MDD + BD-Dep) displayed increased GSCORR relative to HC ($t = 3.35$, $p < 0.001$, FDR-corrected) in transmodal networks such as DMN and FPN, along with reduced GSCORR in unimodal visual regions.

Separate contrasts yielded the same pattern for MDD vs. HC and BD-Dep vs. HC ($t = 2.50$, $p = 0.005$, FDR-corrected), whereas no significant differences emerged between MDD and BD-Dep under identical thresholds (Fig. 1B).

Overall, voxel-wise results indicate a shared Core–Periphery imbalance in both depressive groups relative to healthy controls, with no detectable topographic differences between MDD and BD-Dep.

4.1.2. Single subject prediction - support vector machine group classification using GSCORR maps

We tested whether voxel-wise GSCORR topography could predict individual group membership using SVM multivariate pattern analysis in PRONTO. For MDD vs. HC, the classifier achieved a balanced

accuracy (BA) of 79% ($p = 0.0002$), with sensitivity 82.86%, specificity 75.71%, and AUC = 89%. For BD-Dep vs. HC, performance was similarly robust (BA = 77%, p = 0.0002; sensitivity 82.86%; specificity 71.43%; AUC = 83%).

These results significantly exceeded chance, indicating that altered GSCORR patterns reliably distinguish depressive groups from healthy controls (Schrouff et al., 2016).

To facilitate interpretation of the multivariate classification results, voxel-wise SVM weight maps were computed and are reported in the Supplementary Material (Fig. S2). As expected for multivariate models, these maps represent distributed discriminative patterns rather than independent voxel-wise effects.

4.1.3. Core-periphery topography of depression

The 2 (Topography: Core vs. Periphery) × 3 (Group: MDD, BD-Dep, HC) ANCOVA, controlling for age, sex, and education showed a significant Topography × Group interaction, $F = 4.65$, $p = 0.011$, $\eta^2_p = 0.044$, indicating that the Core–Periphery difference in GSCORR varied across groups. Post hoc tests showed that, although Core values were lower than Periphery in all groups (all $p < 0.001$), this difference was reduced in both MDD and BD-Dep relative to HC (Fig. 2A).

Between-group comparisons further clarified these effects. In Core regions, both MDD and BD-Dep groups exhibited significantly higher GSCORR values compared to HC ($p < 0.001$), while no significant difference was observed between MDD and BD-Dep ($p = 0.81$). In contrast, no significant group differences were found in the Periphery network. These findings suggest that the significant interaction was driven primarily by increased activity in Core networks in the depression groups, while Periphery activity remained comparable across groups (Fig. 2B).

Although a main effect of topography was also observed, $F = 14.38$, $p < 0.001$, $\eta^2_p = 0.07$—indicating generally lower GSCORR values in Core regions compared to Periphery—and the main effect of group was not significant ($F = 1.35$, $p = 0.261$), these effects are secondary in interpretative weight due to the presence of the significant interaction.

So far, the data suggest a Core–Periphery (C–P) topographic reorganization in both MDD and BD-Dep relative to HC. A key question that arises is whether this reflects an abnormal relationship between Core and Periphery activity levels in the two depression groups. To address this, a ratio metric, referred to as the C–P Ratio, was computed to quantify the relative balance between Core and Periphery GSCORR values. A one-way ANCOVA with age, sex, and education as nuisance covariates, was then conducted to examine group differences in C–P Ratio across MDD, BD-Dep, and HC.

The results revealed a significant group effect, $F = 8.72$, $p < 0.001$, $\eta^2 = 0.079$, indicating that diagnosis accounted for 7.9% of the variance in C–P Ratio values. Post hoc comparisons using the Fisher LSD test showed that both MDD and BD-Dep had significantly elevated C–P Ratio values compared to HC (both $p < 0.001$), consistent with an imbalance favoring transmodal core activity. No significant difference was found between MDD and BD-Dep ($p = 0.806$), further supporting a shared alteration in core–periphery dynamics across depressive disorders (Fig. 2C).

These findings reinforce the view that MDD and BD-Dep are marked by a disruption in large-scale functional network topography, particularly in the form of elevated transmodal core activity and a relative flattening of the normal core–periphery gradient. This alteration may represent a transdiagnostic feature of depression-related pathophysiology.

4.1.4. Testing specific networks in core and periphery for their similarities and differences between groups

So far, we focused on the global Core-Periphery topography of MDD and BD-Dep. This leaves open whether they differ in specific single networks. For that, we now tested group differences in each network of the Core (FPN, DMN, Limbic) and Periphery (Visual, SMN, DAN, VAN) via ANCOVA 7 × 3, again considering age sex, and education as nuisance covariates. A consistent pattern of results emerged, with a significant main effect of network ($F = 8.5$, $p < 0.001$) together with a significant Network*Diagnosis interaction ($F = 3.1$, $p < 0.001$). MDD and BD-Dep exhibited substantially higher GSCORR across most of the Core Networks. Specifically, MDD patients showed higher GSCORR in FPN (LSD $p = 0.001$), as well as in DMN (LSD $p \leq 0.001$), while the difference did not reach significance for the Limbic network (LSD $p = 0.226$). The comparison of the three Core networks between BD-Dep and HC returned a similar pattern of results, with the former showing greater GSCORR values in FPN (LSD $p < 0.001$), DMN (LSD $p < 0.001$), yet GSCORR measures are similar in Limbic network among the two groups (LSD $p = 0.178$) (Fig. 3A). Considering the Periphery networks, we obtained overlapping findings when considering MDD and BD against HC. Indeed, MDD patients exhibited reduced GSCORR compared to HC in Visual (LDS $p < 0.001$) and SMN (LSD $p = 0.027$), yet differences were no longer significant for DAN (LSD $p = 0.875$). An opposite trend was observed for VAN, with MDD exhibiting greater GSCORR compared to HC (LSD $p < 0.001$). Partially overlapping with the above, BD-Dep showed lower GSCORR values in Visual Network (LSD $p = 0.002$), while differences no longer exist for SMN (LSD $p = 0.119$). DAN GSCORR were comparable in the two groups (LSD $p = 0.302$), while VAN GSCORR were substantially higher in the clinical group compared to HC (LSD $p < 0.001$). We detected no main effect of Diagnosis ($F = 1.03$, $p = 0.359$) (Fig. 3B).

Overall, our data show an abnormal GSCORR increase in the Core networks, especially in DMN and FPN for MDD and BD, while a decreased GSCORR can be observed in Periphery networks such as Visual and Somatomotor networks (Fig. 3C).

4.1.5. Are the global topographic changes in core and periphery related to depressive symptoms?

We investigated the correlation between GSCORR values of Core and Periphery networks with depressive symptoms as measured by BDI. Partial correlations corrected for age, sex and education revealed a significant negative association of Periphery GSCORR with BDI ($r = -0.229$, $p = 0.013$), while no correlation was found for Core GSCORR and BDI ($r = -0.05$, $p = 0.606$).

The same pattern of correlation was also found for single networks in the Periphery, like Visual Network ($r = -0.2$, $p = 0.031$), SMN ($r = -0.22$, $p = 0.015$), and DA ($r = -0.2$, $p = 0.028$). Together, these findings show a clear relationship of lower GSCORR representation in Periphery networks with the severity of depressive symptomatology (Table S2s). Consistent with these findings Core-Periphery (C–P) ratio was not significantly associated with BDI ($r = -0.15$, $p = 0.11$), indicating that while Periphery network disengagement scales with symptom burden, the C–P Ratio primarily reflects a state-related imbalance between transmodal and unimodal systems rather than a dimensional marker of clinical severity (Table S2).

4.1.6. Global topographic changes in core and periphery in BD mania

To further support the specificity of the Core–Periphery (C–P) imbalance observed in depression (MDD and BD-Dep), we included a sample of individuals with bipolar disorder experiencing a manic episode (BD-Man, $N = 22$). Analyses were first conducted on Core and Periphery GSCORR values and, in a second step, extended to individual resting-state networks. A 2 (Topography: Core, Periphery) × 4 (Group: MDD, BD-Dep, BD-Man, HC) mixed-model ANCOVA revealed a significant topography-by-group interaction ($F = 5.23$, $p < 0.002$). In addition to previously documented differences between depressed and healthy participants, post hoc LSD tests showed that individuals in the manic group exhibited significantly higher GSCORR in the Periphery compared to the MDD group ($p = 0.034$) but did not differ from BD-Dep ($p = 0.118$) or HC participants ($p = 0.212$). No significant group differences were observed in Core regions.

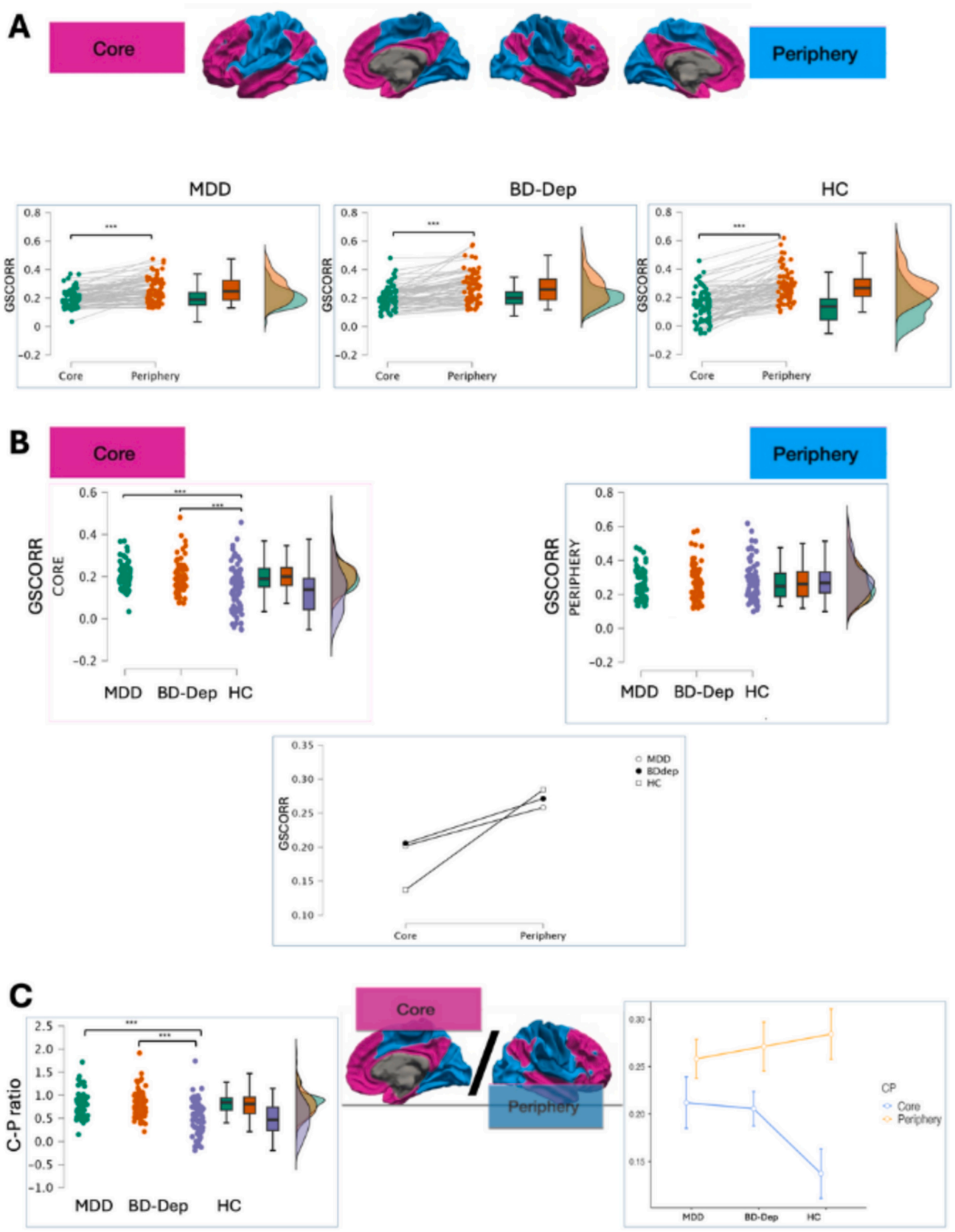

Fig. 2. Visual representation of Core-Periphery (C–P) topography. A) global signal correlation (GSCORR) C–P difference in Major Depressive Disorder (MDD), Bipolar Disorder in Depressive state (BD-Dep) and Healthy Controls (HC). B) Independent comparisons of GSCORR Core and Periphery across groups: MDD vs. HC; BD-Dep vs. HC and MDD vs. BD-Dep. C) C–P Ratio: differences between groups. *** = $p < 0.001$.

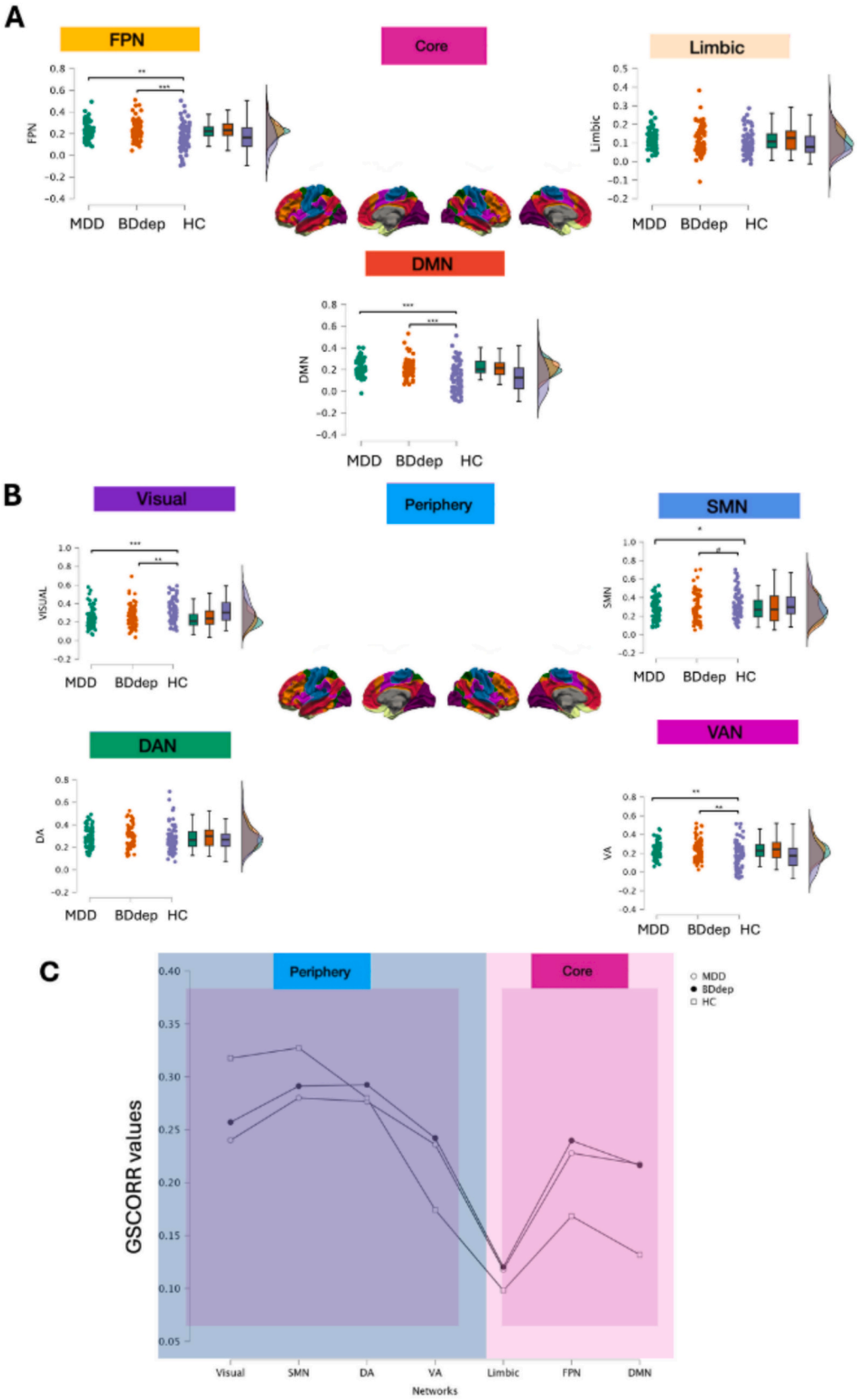

Fig. 3. Visual representation of topography for each network of Core (FPN, DMN and Limbic) and Periphery (Visual, SMN, DA, VA). A) Independent comparisons of GSCORR Core across groups: MDD vs. HC; BD-Dep vs. HC and MDD vs. BD-Dep. B) Independent comparisons of GSCORR Periphery across groups: C) Visual Representation of GSCORR values of MDD, BD-Dep and HC in a Periphery and Core grid.
*** = $p < 0.001$; ** = $p < 0.005$; * = $p < 0.01$; # = $p < 0.05$.

4.1.7. Testing specific networks in core and periphery in BD mania

To provide a more detailed characterization of topographic reorganization across mood states, we conducted a 7 (Network: DMN, FPN, Limbic, Visual, SMN, DA, VA) × 4 (Group: MDD, BD-Dep, BD-Man, HC) mixed-model ANCOVA, again correcting for age, sex, and education. This analysis revealed a significant network-by-group interaction ($F = 3.35$, $p < 0.001$). Manic patients showed significantly elevated GSCORR in the Visual Network compared to both MDD ($p = 0.002$) and BD-Dep ($p = 0.013$) but not compared to healthy controls ($p = 0.238$). A similar pattern was observed in the Somatomotor Network (SMN), where manic patients exhibited higher GSCORR relative to MDD ($p = 0.013$) and BD-Dep ($p = 0.039$). For the Ventral Attention Network (VA), manic individuals also showed increased GSCORR compared to healthy controls ($p = 0.002$), though no significant differences were found between manic and depressed participants. In contrast, no group differences were observed within Core networks (DMN, FPN, Limbic). (Descriptive statistics for these analyses are provided in Supplementary Table S7, Fig. S5).

Finally, to further explore group differences in C–P balance, a one-way ANCOVA was performed on the C–P Ratio. A significant main effect of diagnosis emerged ($F = 7.46$, $p < 0.001$). Post hoc comparisons revealed that both BD-Dep and MDD groups had significantly higher C–P Ratio values than the BD-Man group (BD-Dep: $p = 0.033$; MDD: $p = 0.022$). Additionally, healthy controls exhibited lower C–P Ratio values relative to manic patients ($p = 0.043$). (See Fig. 4 for a visual representation overview of findings including MDD, BD-Dep, HC and BD-mania).

4.1.8. Partial least squares discriminating mood states

Lastly, to assess the multivariate discriminability of brain-wide GSCORR patterns across diagnostic groups, a Partial Least Squares (PLS) analysis was conducted to distinguish between BD-Man, BD-Dep, MDD, and HC.

A Core-Periphery topography with proportionally higher values for global Core and Core-related specific networks predicted group assignment to MDD or BD-Dep; while proportionally higher values for global Periphery and Periphery-related specific networks predicted group assignment to HC or BD-Man (see Fig. 5).

A PLS linear regression, with measures of Core-Periphery (Core, Periphery, and C–P ratio) and specific network (DMN, FPN, Limbic, Visual, SMN, DA, VA) topography as predictors of diagnosis, defined a model with one significant component (coefficient = 0.289) explaining 7.2% of variance in diagnostic assignment, by using 37.5% of the variance in the predictor variables ($R^2X = 0.375$; $R^2Y = 0.072$; $Q^2 = 0.046$). The variable selected as the most relevant to predict diagnosis was the C–P ratio (VIP = 1.65), followed by a significant effect of DMN (VIP = 1.35), Core (VIP = 1.29), FPN (VIP = 1.09) and Visual (VIP = 1.01), with VA, Limbic, SMN, Periphery, and DA showing a VIP < 1.The analysis of predictive weights (w) showed that the contribution of single factors to the latent variable, to predict diagnosis, was in opposite direction for predictors related to a higher Core topography (Core w = 0.408, C–P ratio w = 0.523, DMN = 0.428, FPN w = 0.346, Limbic w = 0.184), and for predictors related to a higher Periphery topography (Periphery w = −0.116, Visual w = −0.318, SMN w = −0.170), with two exceptions however related to non-significant factors (DA w = 0.022, VA w = 0.281).

Analysis of Y loadings showed that the latent variable, resulting from the above Core-Periphery topography, had positive effects of similar strength in predicting group assignment to depression (MDD = 0.435, BD-Dep = 0.427), with opposite effects to predict the HC (−0.783) and BD-Man (−0.124) conditions.

Based on the above, we then repeated the PLS linear regression after grouping together depressed (MDD + BD-Dep) and non-depressed (HC + BD-Man) participants. The model improved its predictive power, by increasing its level of significance ($Q^2 = 0.14$) and its coefficient of determination, becoming able to explain 19.4% of variance, by using a similar 36.3% variance in predictors ($R^2X = 0.363$; $R^2Y = 0.194$). Again, C–P ratio was the main predictor, with significant contributions of DMN, Core Visual, and FPN. Predictive weights and Y loadings did not change directions.

Excluding manic patients, and testing depressed patients (MDD + BD-Dep) against HC, further improved the coefficient of determination ($R^2Y = 0.210$), leaving the model effects unchanged.

Finally, a model with this same set of predictors was unable to provide a significant solution for differentiating group assignment to MDD vs BD-Dep, using a large proportion of variance in predictors to explain a negligible proportion of variance in the dependent variable ($R^2X = 0.561$; $R^2Y = 0.006$; $Q^2 = -0.103$).

5. Discussion

5.1. Topographic reorganization in depression of both MDD and BD-Dep in fMRI

We show a topographic reorganization of transmodal-core and unimodal-periphery networks in both MDD and BD-Dep, with a shift toward core regions and reduced periphery engagement. This converges with prior evidence of similar reorganization in acute MDD (Northoff and Hirjak, 2024; Scalabrini et al., 2020) and its 'normalization' in response to pharmacological (Abdallah et al., 2017; Zhu et al., 2019; Kraus et al., 2020; Long et al., 2023; van de Ven et al., 2013; Zhang et al., 2020), stimulation (Kong et al., 2023; Zhang et al., 2021) and psychotherapeutic (Long et al., 2023) interventions.

Extending this work to BD, our findings, together with reports of increased activity/connectivity in transmodal DMN regions (Martino et al., 2020; Martino et al., 2016; Yang et al., 2021) and decreased engagement of unimodal sensory–motor cortices (Martino et al., 2020; Martino et al., 2016; Northoff et al., 2018; Zhang et al., 2019), suggest that core–periphery imbalance may represent a shared neural marker of depressive states across diagnoses.

Taken together, these findings indicate that, at the macroscale level of global signal topography, depressive states share a common organizational signature across diagnostic categories, whereas disorder-specific differences may become evident at finer levels of analysis. Such common network alterations may help explain overlapping clinical features of MDD and BD depression, including excessive rumination, heightened self-focus, persistent negative mood, and psychomotor retardation (Scalabrini et al., 2025a; Song et al., 2024a; Zhang et al., 2019; Davey and Harrison, 2022; Grimm et al., 2009; Grimm et al., 2011; Hamilton et al., 2015; Keskin et al., 2023; Nejad et al., 2013; Zhou et al., 2020).

Importantly, increased coupling within the Core should not be interpreted as reflecting a single cognitive process restricted to self-referential mentation. The Core networks considered here (including the DMN, FPN, and limbic systems) collectively support a broad range of transmodal and internally oriented functions, such as autobiographical memory retrieval, future-oriented simulation, emotional appraisal, and higher-order cognitive control (Buckner et al., 2008; Spreng et al., 2010; Zanto and Gazzaley, 2013). Within this framework, the DMN has been consistently implicated in memory-based and prospective cognition (Buckner et al., 2008; Schacter et al., 2012), the frontoparietal network in the regulation and monitoring of internally generated mental content (Spreng et al., 2010; Dixon et al., 2018), and limbic regions in affective salience and emotional integration (Pessoa et al., 2012). While DMN and frontoparietal contributions were robust across analyses, limbic involvement appeared more variable, suggesting greater state-dependence of affective components. Accordingly, the observed shift toward the Core is best understood as a large-scale reorganization favoring internally oriented, abstract, and temporally extended modes of cognition, rather than selective amplification of any single cognitive function.

Intriguingly, while the shift toward Core networks highlights their

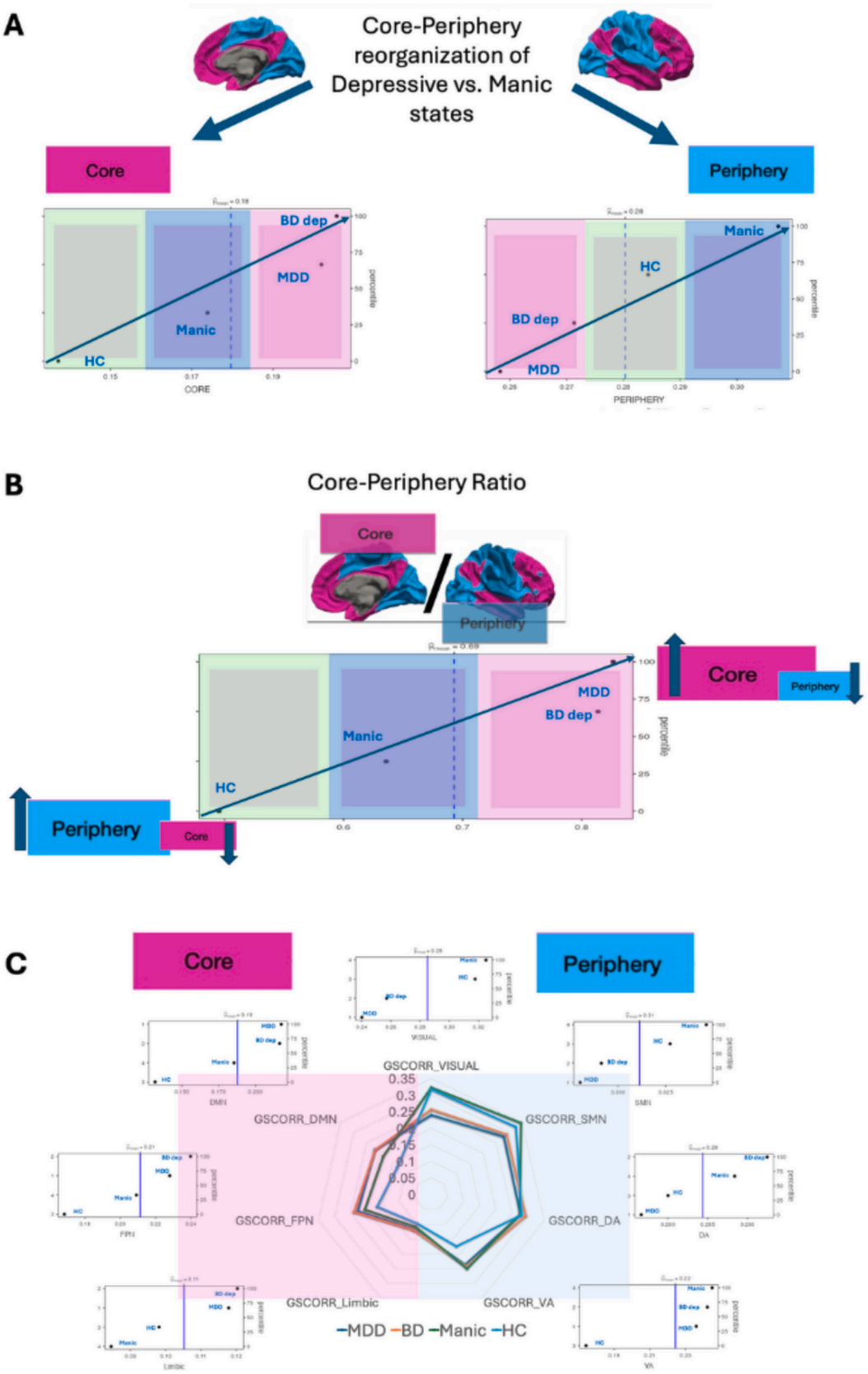

Fig. 4. Visual representation trough dot-plots to examine the global topographic reorganization in the different groups (MDD, BD-Dep, HC and BD-Manic). A) Global topographic re-organization in Core and Periphery. B) Global topographic re-organization for C–P Ratio. C) Gobal topographic re-organization for each network of Core (DMN, FPN, Limbic) and Periphery (Visual, SMN, DA and VA).

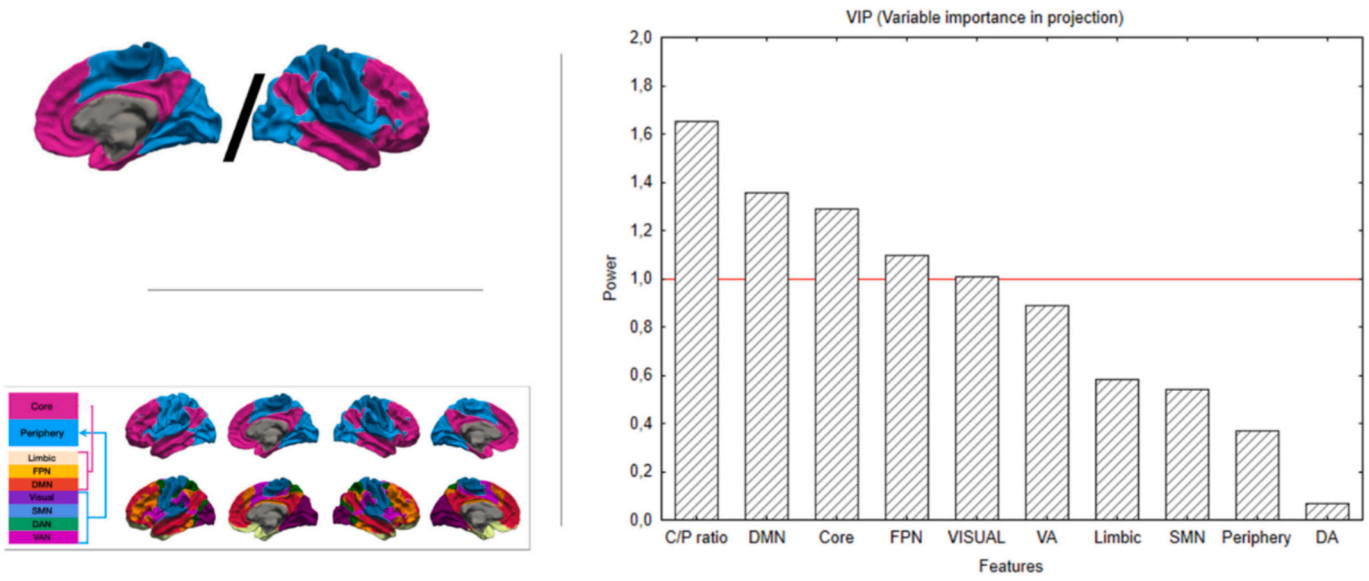

Fig. 5. Visual Representation of Variable Importance in Projection (VIP) scores derived from Partial Least Squares (PLS) analysis, illustrating the relative contribution of each feature to the diagnostic model. Features with VIP scores greater than 1 are considered the most influential in predicting diagnostic outcomes.

central role, our data also underscore the relevance of Periphery systems. The Core–Periphery (C–P) Ratio differentiated diagnostic groups, and Periphery GSCORR showed a significant negative association with depressive severity, indicating that reduced Periphery representation relates to more severe symptoms. This is consistent with evidence implicating sensory–motor and visual networks in mood disorders. These networks support basic sensory processing and bodily regulation, and their disruption reflects broader alterations in perceptual and motor functions in depression. Liu et al. (Liu et al., 2022) and Song et al. (Song et al., 2024b) observed that in individuals with depression, activity in visual and sensory-motor cortices was often diminished, which is associated with emotional blunting and psychomotor retardation. Similarly, Scalabrini et al. (Scalabrini et al., 2025a) reported abnormally slow and desynchronized visual cortical activity linked to greater symptom severity and altered higher-order connectivity.

These findings are consistent with evidence showing that depression involves disturbances not only in higher-order cognition but also in basic sensory and motor processing (Hu et al., 2024; Zhang et al., 2025). Accordingly, core–periphery imbalance may reflect a broader dysregulation of both externally oriented sensory processes and internally oriented cognitive–emotional functions that jointly shape depressive symptomatology. Our results therefore highlight the relevance of considering disruptions in both network classes, with the C–P Ratio offering a useful large-scale marker. While traditional models emphasize cognitive and emotional regulation, our data underscore the contribution of periphery systems to symptom severity. Future studies should clarify how these imbalances evolve and whether they are modifiable through treatment.

Finally, our proof-of-concept analysis of BD mania showed a distinct topographic pattern compared to BD-Dep and MDD, with greater globally mediated connectivity in unimodal-periphery regions. Although based on a smaller sample, this suggests an opposite network configuration during mania relative to depression, consistent with prior reports of contrasting network balances across BD mood states (Martino et al., 2016).

Further supporting the topographical findings, machine learning analyses showed that altered GSCORR topography reliably distinguished both MDD and BD-Dep from healthy controls (HC), with balanced accuracies of 79% for MDD vs. HC and 77% for BD-Dep vs. HC, and AUCs of 89% and 83%, respectively. PLS analysis corroborated these effects by identifying a latent pattern of GSCORR variability that differentiated depressive and manic states as well as HC. The proportion of diagnostic variance explained exceeded 20% when comparing depressed participants (MDD + BD-Dep) to HC, underscoring that distributed large-scale features carry meaningful state-related information.

The emergence of the Core–Periphery Ratio as the most predictive feature reinforces our central conclusion: mood disorders may be better characterized by large-scale network imbalances than by isolated regional abnormalities. The prominence of DMN, FPN, and Visual networks in the VIP analysis is consistent with their roles in self-referential processing and emotional regulation (Raichle et al., 2001; Greicius et al., 2003), executive control and cognitive flexibility (Dosenbach et al., 2008), and perceptual processing of emotionally salient stimuli (Vuilleumier, 2005).

These findings align with literature indicating that disruptions in macroscale functional architecture (particularly the balance between transmodal hubs and unimodal systems) contribute to dysregulated emotion, impaired cognitive control, and altered self-referential thinking in mood disorders (Menon, 2011; Seeley et al., 2007; Yeo et al., 2011b). Imbalances between core and periphery networks may therefore represent a systems-level mechanism underlying depressive and manic psychopathology (Cole et al., 2014; Crossley et al., 2014).

Still in its infancy, a growing line of research is beginning to identify fine-grained rsfMRI differences that help distinguish BD from MDD during depressive episodes. Such work has highlighted alterations in cortico-limbic-striatal circuits, components of reward and aversion pathways, and regions within the DMN (e.g., ventral striatum, periacqueductal gray, anterior cingulate cortex, prefrontal cortex, insula, hippocampus) (Calesella et al., 2024), with some studies linking specific psychopathological dimensions to distinct neural regions or networks (Redlich et al., 2015).

At the same time, the phenomenology of depression points to a fundamental experiential disruption, one that shapes emotional life and responsivity to stimuli, even if its mechanisms remain inaccessible to awareness (Schneider, 1949). A sparse literature suggests that this key vital change can be partly revealed by studies of the biological correlates of cognitive vulnerability, such as time generation, interoception, and other dimensions that surpass the possibility of awareness (Elliott et al., 2002; Erickson et al., 2005; Yoshiike et al., 2020). We propose that examining global brain-signal topography, as a marker of system-level dysregulation, may help capture these foundational aspects of

depressive experience, supporting the view of depression as a disorder of global dynamic reorganization (Northoff and Hirjak, 2024).

Future work should assess whether the Core–Periphery imbalance identified here in MDD and BD-Dep extends to other forms of depressive psychopathology, including postpartum, schizoaffective, and medically related depression.

In conclusion, our data suggests that Core–Periphery (C–P) imbalance may serve as a dynamic neural marker reflecting shifts along the mood continuum. This dynamic perspective aligns with emerging models that conceptualize mood disorders as fluctuating disruptions within large-scale network organization rather than fixed regional abnormalities. It supports the notion that cognitive-affective-sensory states are associated with shifting patterns of integration and segregation across functional networks, particularly between transmodal-core regions and unimodal-peripheral systems (Deco et al., 2015; Shine et al., 2019).

Taken together, these findings argue for a conceptual shift toward viewing mood pathology through the lens of global-system level dysregulation, rather than as static, region-specific dysfunction. This global-systems level framework may help bridge phenomenological observations of mood lability with measurable neural dynamics, offering novel pathways for understanding and potentially treating mood disorders.

5.2. Theoretical integration with network-dynamics frameworks

We interpret the observed Core–Periphery imbalance in global signal topography as a form of system-level dysregulation grounded in spatiotemporal neuroscience, whereby spatial gradients (unimodal–transmodal / periphery–core) are coupled with temporal hierarchies (short–long intrinsic timescales) that constrain large-scale integration and segregation (Northoff and Hirjak, 2024; Wolff et al., 2022). Within this framework, depression can be conceived as a topographic–dynamic reorganization in which transmodal core systems (e.g., DMN/FPN and partially limbic circuits) exert abnormally strong global coordination, while unimodal peripheral systems show reduced global coupling, consistent with the idea that global activity is not mere "noise" but carries physiologically meaningful information relevant to psychopathology (Northoff and Hirjak, 2024; Schölvinck et al., 2010).

This system-level view aligns naturally with predictive coding / active inference accounts: a shift toward core regions may reflect an over-weighting of higher-order priors and internally generated models (supported by long timescales and strong transmodal integration), alongside reduced precision or impact of sensory prediction errors in unimodal systems, yielding diminished peripheral engagement and a bias toward internally oriented cognition (Clark, 2013; Friston, 2010; Seth and Friston, 2016). In this sense, Core–Periphery imbalance provides a macroscale neural signature consistent with aberrant hierarchical inference, potentially linking global topography to clinical phenomena such as rumination, altered self-related processing, and reduced sensory–motor reactivity.

Finally, the findings are also compatible (at a more abstract level) with global workspace–type proposals, where conscious access and flexible reportability depend on large-scale broadcasting and integration across frontoparietal/transmodal systems (Baars, 2005; Dehaene et al., 2011; Mashour et al., 2020). Our results do not adjudicate between frameworks, but they support the broader notion that depressive states involve a reconfiguration of global integration architecture, with altered balance between transmodal core hubs and unimodal peripheral systems.

5.3. Limitations

Some limitations should be acknowledged. First, although fMRI provides valuable insight into large-scale topographic organization, its spatial and temporal constraints limit the precision with which dynamic processes can be captured. Nonetheless, the present findings align with prior work (Scalabrini et al., 2020), and extend it by including both depressive and manic states, supporting the robustness of the approach.

Second, the sample derives from a specific clinical cohort, which may limit generalizability. Replication in larger and more demographically diverse populations is needed to confirm the reliability of these results.

Third, while the Core–Periphery imbalance and related topographic features show promise, their clinical utility as biomarkers remains preliminary. Real-world diagnostic contexts involve confounding factors such as medication and comorbidities that were not exhaustively addressed here. Nevertheless, extensive whole brain and network level medication sensitivity analysis (see Supplementary material) indicated that the main findings were robust.

Finally, the BD-Man group was comparatively small due to the inherent difficulties of scanning individuals in manic states. Although included primarily as a proof of principle, this limits statistical power and calls for replication in larger manic samples. Despite this, the BD-Man data offer initial insight into topographic alterations across the mood continuum.

6. Conclusion

This study shows a shared topographic reorganization in MDD and BD-Dep, marked by a shift toward transmodal-core networks and reduced engagement of unimodal-periphery regions, extending previous MDD findings (Scalabrini et al., 2020), to bipolar depression. Machine learning analyses confirmed that altered GSCORR topography reliably distinguishes depressive states from healthy controls.

Our results also emphasize the contribution of peripheral networks, particularly visual and sensory-motor systems, to depressive severity, supporting the view that depression involves disruptions in both cognitive and basic sensory–motor functions (Liu et al., 2022; Song et al., 2024a; Scalabrini et al., 2025b). In contrast, BD mania displayed an opposite pattern, with increased unimodal-periphery and reduced core connectivity, consistent with prior evidence of divergent network balances across mood states. PLS analyses further highlighted the relevance of distributed topographic features, especially the Core–Periphery ratio and activity within DMN, FPN, and Visual networks, reinforcing a global-systems model of mood disorder pathology.

In summary, both core and periphery disruptions appear central to mood disorders. Although topographic abnormalities represent a promising neurobiological marker, the overlap between MDD and BD-Dep underscores the challenges of differential diagnosis. Future work should refine and validate such biomarkers to support more precise and personalized interventions.

CRediT authorship contribution statement

Andrea Scalabrini: Writing – review & editing, Writing – original draft, Visualization, Validation, Methodology, Investigation, Formal analysis, Conceptualization. **Mariagrazia Palladini:** Writing – review & editing, Formal analysis. **Sara Poletti:** Writing – review & editing, Validation, Resources, Methodology, Formal analysis, Data curation. **Benedetta Vai:** Writing – review & editing, Resources, Data curation. **Federico Calesella:** Software, Formal analysis. **Marco Paolini:** Methodology, Investigation. **Giulia Gulino:** Formal analysis. **Sara Masoumi:** Writing – review & editing, Conceptualization. **Raffaella Zanardi:** Writing – review & editing, Investigation, Data curation. **Cristina Colombo:** Validation, Data curation. **Georg Northoff:** Writing – review & editing, Supervision, Conceptualization. **Francesco Benedetti:** Writing – review & editing, Supervision, Investigation, Funding acquisition, Data curation, Conceptualization.

Ethics approval

All procedures performed in studies involving human participants were in accordance with the ethical standards of the local ethics

committee and with the 1964 Helsinki declaration and its later amendments. Written informed consent was obtained from all participants prior to inclusion in the study.

Funding

Funded by the European Union—Next Generation EU NRRP M6C2—Investment 2.1. Enhancement and strengthening of biomedical research in the NHS—Italian Ministry of Health, BANDO PNRR -PNRR23-8015 MCNT2-2023-12378015.CUP C43C24000250007 (FB).

Declaration of competing interest

The authors declare that they have no known competing financial or personal interests that could have appeared to influence the work reported in this manuscript.

Acknowledgements

None.

Appendix A. Supplementary data

Supplementary data to this article can be found online at https://doi.org/10.1016/j.jad.2026.121550.

Data availability

Due to ethical and privacy restrictions involving clinical and neuroimaging data from human participants, datasets are not publicly available. Anonymized data and analytical code may be requested from the corresponding author, subject to institutional regulations and ethics committee approval.

References

Abdallah, C.G., Averill, L.A., Collins, K.A., Geha, P., Schwartz, J., Averill, C., et al., 2017. Ketamine treatment and global brain connectivity in major depression. Neuropsychopharmacology 42 (6), 1210–1219.
Akarachantachote, N., Chadcham, S., Saithanu, K., 2014. Cutoff threshold of variable importance in projection for variable selection. Int. J. Pure Appl. Math. 94 (3), 307–322.
Ao, Y., Ouyang, Y., Yang, C., Wang, Y., 2021. Global signal topography of the human brain: a novel framework of functional connectivity for psychological and pathological investigations. Front. Hum. Neurosci. 15, 644892.
Baars, B.J., 2005. Global workspace theory of consciousness: toward a cognitive neuroscience of human experience. Prog. Brain Res. 150, 45–53.
Berger, H., 1929. Über das elektroenkephalogramm des menschen. Arch. Psychiatr. Nervenkr. 87 (1), 527–570.
Bravi, B., Verga, C., Palladini, M., Poletti, S., Buticchi, C., Stefania, S., et al., 2025. Effects of kynurenine pathway metabolites on choroid plexus volume, hemodynamic response, and spontaneous neural activity: a new mechanism for disrupted neurovascular communication and impaired cognition in mood disorders. Brain Behav. Immun. 125, 414–427.
Buckner, R.L., Andrews-Hanna, J.R., Schacter, D.L., 2008. The brain's default network: anatomy, function, and relevance to disease. Ann. N. Y. Acad. Sci. 1124 (1), 1–38.
Calesella, F., Colombo, F., Bravi, B., Fortaner-Uyà, L., Monopoli, C., Poletti, S., et al., 2024. A machine learning pipeline for efficient differentiation between bipolar and major depressive disorder based on multimodal structural neuroimaging. Neurosci. Appl. 3, 103931.
Clark, A., 2013. Whatever next? Predictive brains, situated agents, and the future of cognitive science. Behav. Brain Sci. 36 (3), 181–204.
Cole, M.W., Bassett, D.S., Power, J.D., Braver, T.S., Petersen, S.E., 2014. Intrinsic and task-evoked network architectures of the human brain. Neuron 83 (1), 238–251.
Crossley, N.A., Mechelli, A., Scott, J., Carletti, F., Fox, P.T., McGuire, P., et al., 2014. The hubs of the human connectome are generally implicated in the anatomy of brain disorders. Brain 137 (8), 2382–2395.
Cuellar, A.K., Johnson, S.L., Winters, R., 2005. Distinctions between bipolar and unipolar depression. Clin. Psychol. Rev. 25 (3), 307–339.
Davey, C.G., Harrison, B.J., 2022. The self on its axis: a framework for understanding depression. Transl. Psychiatry 12 (1), 23.
Davey, C.G., Pujol, J., Harrison, B.J., 2016. Mapping the self in the brain's default mode network. Neuroimage 132, 390–397.
Deco, G., Tononi, G., Boly, M., Kringelbach, M.L., 2015. Rethinking segregation and integration: contributions of whole-brain modelling. Nat. Rev. Neurosci. 16 (7), 430–439.
Dehaene, S., Changeux, J.-P., Naccache, L., 2011. The global neuronal workspace model of conscious access: from neuronal architectures to clinical applications. In: Characterizing Consciousness: From Cognition to the Clinic?, pp. 55–84.
Dixon, M.L., De La Vega, A., Mills, C., Andrews-Hanna, J., Spreng, R.N., Cole, M.W., et al., 2018. Heterogeneity within the frontoparietal control network and its relationship to the default and dorsal attention networks. Proc. Natl. Acad. Sci. 115 (7). E1598-E607.
Dosenbach, N.U., Fair, D.A., Cohen, A.L., Schlaggar, B.L., Petersen, S.E., 2008. A dual-networks architecture of top-down control. Trends Cogn. Sci. 12 (3), 99–105.
Doucet, G.E., Janiri, D., Howard, R., O'Brien, M., Andrews-Hanna, J.R., Frangou, S., 2020. Transdiagnostic and disease-specific abnormalities in the default-mode network hubs in psychiatric disorders: a meta-analysis of resting-state functional imaging studies. Eur. Psychiatry 63 (1), e57.
Elliott, R., Rubinsztein, J.S., Sahakian, B.J., Dolan, R.J., 2002. The neural basis of mood-congruent processing biases in depression. Arch. Gen. Psychiatry 59 (7), 597–604.
Erickson, K., Drevets, W.C., Clark, L., Cannon, D.M., Bain, E.E., Zarate Jr., C.A., et al., 2005. Mood-congruent bias in affective go/no-go performance of unmedicated patients with major depressive disorder. Am. J. Psychiatry 162 (11), 2171–2173.
Friston, K., 2010. The free-energy principle: a unified brain theory? Nat. Rev. Neurosci. 11 (2), 127–138.
Greicius, M.D., Krasnow, B., Reiss, A.L., Menon, V., 2003. Functional connectivity in the resting brain: a network analysis of the default mode hypothesis. Proc. Natl. Acad. Sci. 100 (1), 253–258.
Grimm, S., Boesiger, P., Beck, J., Schuepbach, D., Bermpohl, F., Walter, M., et al., 2009. Altered negative BOLD responses in the default-mode network during emotion processing in depressed subjects. Neuropsychopharmacology 34 (4), 932–943.
Grimm, S., Ernst, J., Boesiger, P., Schuepbach, D., Boeker, H., Northoff, G., 2011. Reduced negative BOLD responses in the default-mode network and increased self-focus in depression. World J. Biol. Psychiatry 12 (8), 627–637.
Hamilton, J.P., Furman, D.J., Chang, C., Thomason, M.E., Dennis, E., Gotlib, I.H., 2011. Default-mode and task-positive network activity in major depressive disorder: implications for adaptive and maladaptive rumination. Biol. Psychiatry 70 (4), 327–333.
Hamilton, J.P., Etkin, A., Furman, D.J., Lemus, M.G., Johnson, R.F., Gotlib, I.H., 2012. Functional neuroimaging of major depressive disorder: a meta-analysis and new integration of baseline activation and neural response data. Am. J. Psychiatry 169 (7), 693–703.
Hamilton, J.P., Farmer, M., Fogelman, P., Gotlib, I.H., 2015. Depressive rumination, the default-mode network, and the dark matter of clinical neuroscience. Biol. Psychiatry 78 (4), 224–230.
Hao, Z.Y., Zhong, Y., Ma, Z.J., Xu, H.Z., Kong, J.Y., Wu, Z., et al., 2020. Abnormal resting-state functional connectivity of hippocampal subfields in patients with major depressive disorder. BMC Psychiatry 20, 1–11.
Hu, Y., Li, S., Li, J., Zhao, Y., Li, M., Cui, W., et al., 2024. Impaired visual-motor functional connectivity in first-episode medication-naïve patients with major depressive disorder. Cereb. Cortex 34 (1), bhad387.
Janiri, D., Frangou, S., 2022. Precision neuroimaging biomarkers for bipolar disorder. Int. Rev. Psychiatry 34 (7–8), 727–735.
Kaiser, R.H., Andrews-Hanna, J.R., Wager, T.D., Pizzagalli, D.A., 2015. Large-scale network dysfunction in major depressive disorder: a meta-analysis of resting-state functional connectivity. JAMA Psychiatry 72 (6), 603–611.
Keskin, K., Eker, M.Ç., Gönül, A.S., Northoff, G., 2023. Abnormal global signal topography of self modulates emotion dysregulation in major depressive disorder. Transl. Psychiatry 13 (1), 107.
Kong, Y., Zhou, J., Zhao, M., Zhang, Y., Tan, T., Xu, Z., et al., 2023. Non-inferiority of intermittent theta burst stimulation over the left V1 vs. classical target for depression: a randomized, double-blind trial. J. Affect. Disord. 343, 59–70.
Kraus, C., Mkrtchian, A., Kadriu, B., Nugent, A.C., Zarate Jr., C.A., Evans, J.W., 2020. Evaluating global brain connectivity as an imaging marker for depression: influence of preprocessing strategies and placebo-controlled ketamine treatment. Neuropsychopharmacology 45 (6), 982–989.
Liu, T.T., Nalci, A., Falahpour, M., 2017. The global signal in fMRI: nuisance or information? Neuroimage 150, 213–229.
Liu, D.-Y., Ju, X., Gao, Y., Han, J.-F., Li, Z., Hu, X.-W., et al., 2022. From molecular to behavior: higher order occipital cortex in major depressive disorder. Cereb. Cortex 32 (10), 2129–2139.
Long, Z., Chen, D., Lei, X., 2023. Enhanced rich club connectivity in mild or moderate depression after nonpharmacological treatment: a preliminary study. Brain Behav. 13 (10), e3198.
Lu, X., Zhang, J.-F., Gu, F., Zhang, H.-x., Zhang, M., Zhang, H.-s., et al., 2022. Altered task modulation of global signal topography in the default-mode network of unmedicated major depressive disorder. J. Affect. Disord. 297, 53–61.
Martino, M., Magioncalda, P., Huang, Z., Conio, B., Piaggio, N., Duncan, N.W., et al., 2016. Contrasting variability patterns in the default mode and sensorimotor networks balance in bipolar depression and mania. Proc. Natl. Acad. Sci. 113 (17), 4824–4829.
Martino, M., Magioncalda, P., Conio, B., Capobianco, L., Russo, D., Adavastro, G., et al., 2020. Abnormal functional relationship of sensorimotor network with neurotransmitter-related nuclei via subcortical-cortical loops in manic and depressive phases of bipolar disorder. Schizophr. Bull. 46 (1), 163–174.
Mashour, G.A., Roelfsema, P., Changeux, J.-P., Dehaene, S., 2020. Conscious processing and the global neuronal workspace hypothesis. Neuron 105 (5), 776–798.

Menon, V., 2011. Large-scale brain networks and psychopathology: a unifying triple network model. Trends Cogn. Sci. 15 (10), 483–506.
Murphy, K., Fox, M.D., 2017. Towards a consensus regarding global signal regression for resting state functional connectivity MRI. Neuroimage 154, 169–173.
Murrough, J.W., Abdallah, C.G., Anticevic, A., Collins, K.A., Geha, P., Averill, L.A., et al., 2016. Reduced global functional connectivity of the medial prefrontal cortex in major depressive disorder. Hum. Brain Mapp. 37 (9), 3214–3223.
Nejad, A.B., Fossati, P., Lemogne, C., 2013. Self-referential processing, rumination, and cortical midline structures in major depression. Front. Hum. Neurosci. 7, 666.
Northoff, G., 2007. Psychopathology and pathophysiology of the self in depression—neuropsychiatric hypothesis. J. Affect. Disord. 104 (1–3), 1–14.
Northoff, G., 2016a. Is the self a higher-order or fundamental function of the brain? The "basis model of self-specificity" and its encoding by the brain's spontaneous activity. Cogn. Neurosci. 7 (1–4), 203–222.
Northoff, G., 2016b. Spatiotemporal psychopathology I: no rest for the brain's resting state activity in depression? Spatiotemporal psychopathology of depressive symptoms. J. Affect. Disord. 190, 854–866.
Northoff, G., 2024. Beyond mood—depression as a speed disorder: biomarkers for abnormal slowness. J. Psychiatry Neurosci. 49 (5), 357–366.
Northoff, G., Hirjak, D., 2024. Is depression a global brain disorder with topographic dynamic reorganization? Transl. Psychiatry 14 (1), 278.
Northoff, G., Magioncalda, P., Martino, M., Lee, H.-C., Tseng, Y.-C., Lane, T., 2018. Too fast or too slow? Time and neuronal variability in bipolar disorder—a combined theoretical and empirical investigation. Schizophr. Bull. 44 (1), 54–64.
Palermo, G., Piraino, P., Zucht, H.-D., 2009. Performance of PLS regression coefficients in selecting variables for each response of a multivariate PLS for omics-type data. Adv. Appl. Bioinform. Chem. 57–70.
Pessoa, L., Lindquist, K.A., Wager, T.D., Kober, H., Bliss-Moreau, E., Barrett, L.F., 2012. Beyond brain regions: network perspective of cognition–emotion interactions. Behav. Brain Sci. 35 (3), 158.
Power, J.D., Barnes, K.A., Snyder, A.Z., Schlaggar, B.L., Petersen, S.E., 2012. Spurious but systematic correlations in functional connectivity MRI networks arise from subject motion. Neuroimage 59 (3), 2142–2154.
Price, J.L., Drevets, W.C., 2010. Neurocircuitry of mood disorders. Neuropsychopharmacology 35 (1), 192–216.
Quraishi, S., Frangou, S., 2002. Neuropsychology of bipolar disorder: a review. J. Affect. Disord. 72 (3), 209–226.
Raichle, M.E., 2015. The brain's default mode network. Annu. Rev. Neurosci. 38, 433–447.
Raichle, M.E., MacLeod, A.M., Snyder, A.Z., Powers, W.J., Gusnard, D.A., Shulman, G.L., 2001. A default mode of brain function. Proc. Natl. Acad. Sci. 98 (2), 676–682.
Redlich, R., Dohm, K., Grotegerd, D., Opel, N., Zwitserlood, P., Heindel, W., et al., 2015. Reward processing in unipolar and bipolar depression: a functional MRI study. Neuropsychopharmacology 40 (11), 2623–2631.
Scalabrini, A., Vai, B., Poletti, S., Damiani, S., Mucci, C., Colombo, C., et al., 2020. All roads lead to the default-mode network—global source of DMN abnormalities in major depressive disorder. Neuropsychopharmacology 45 (12), 2058–2069.
Scalabrini, A., Poletti, S., Vai, B., Paolini, M., Gao, Y., Hu, Y.-T., et al., 2025a. Abnormally slow dynamics in occipital cortex of depression. J. Affect. Disord. 523–530.
Scalabrini, A., Poletti, S., Vai, B., Paolini, M., Gao, Y., Hu, Y.-T., et al., 2025b. Abnormally slow dynamics in occipital cortex of depression. J. Affect. Disord. 374, 523–530.
Schacter, D.L., Addis, D.R., Hassabis, D., Martin, V.C., Spreng, R.N., Szpunar, K.K., 2012. The future of memory: remembering, imagining, and the brain. Neuron 76 (4), 677–694.
Scheinost, D., Holmes, S.E., DellaGioia, N., Schleifer, C., Matuskey, D., Abdallah, C.G., et al., 2018. Multimodal investigation of network level effects using intrinsic functional connectivity, anatomical covariance, and structure-to-function correlations in unmedicated major depressive disorder. Neuropsychopharmacology 43 (5), 1119–1127.
Schneider, K., 1949. Die Untergrundsdepressionen. Fortschr Neurol Psychiatr u Ihre Grenzgebiete. 17, 429–434.
Schölvinck, M.L., Maier, A., Ye, F.Q., Duyn, J.H., Leopold, D.A., 2010. Neural basis of global resting-state fMRI activity. Proc. Natl. Acad. Sci. 107 (22), 10238–10243.
Schrouff, J., Rosa, M.J., Rondina, J.M., Marquand, A.F., Chu, C., Ashburner, J., et al., 2013. PRoNTo: pattern recognition for neuroimaging toolbox. Neuroinformatics 11 (3), 319–337.
Schrouff, J., Mourão-Miranda, J., Phillips, C., Parvizi, J., 2016. Decoding intracranial EEG data with multiple kernel learning method. J. Neurosci. Methods 261, 19–28.
Seeley, W.W., Menon, V., Schatzberg, A.F., Keller, J., Glover, G.H., Kenna, H., et al., 2007. Dissociable intrinsic connectivity networks for salience processing and executive control. J. Neurosci. 27 (9), 2349–2356.
Seth, A.K., Friston, K.J., 2016. Active interoceptive inference and the emotional brain. Philos. Trans. R. Soc. B 371 (1708), 20160007.
Shine, J.M., Breakspear, M., Bell, P.T., Ehgoetz Martens, K.A., Shine, R., Koyejo, O., et al., 2019. Human cognition involves the dynamic integration of neural activity and neuromodulatory systems. Nat. Neurosci. 22 (2), 289–296.
Song, X.M., Hu, X.-W., Li, Z., Gao, Y., Ju, X., Liu, D.-Y., et al., 2021. Reduction of higher-order occipital GABA and impaired visual perception in acute major depressive disorder. Mol. Psychiatry 26 (11), 6747–6755.
Song, X.M., Liu, D.Y., Hirjak, D., Hu, X.W., Han, J.F., Roe, A.W., et al., 2024a. Motor versus psychomotor? Deciphering the neural source of psychomotor retardation in depression. Adv. Sci. 11 (40), 2403063.
Song, X.M., Liu, D.Y., Hirjak, D., Hu, X.W., Han, J.F., Roe, A.W., et al., 2024b. Motor versus psychomotor? Deciphering the neural source of psychomotor retardation in depression. Adv. Sci., 2403063
Spreng, R.N., Stevens, W.D., Chamberlain, J.P., Gilmore, A.W., Schacter, D.L., 2010. Default network activity, coupled with the frontoparietal control network, supports goal-directed cognition. Neuroimage 53 (1), 303–317.
Varoquaux, G., 2018. Cross-validation failure: small sample sizes lead to large error bars. Neuroimage 180 (Pt A), 68–77.
van de Ven, V., Wingen, M., Kuypers, K.P., Ramaekers, J.G., Formisano, E., 2013. Escitalopram decreases cross-regional functional connectivity within the default-mode network. PloS One 8 (6), e68355.
Vuilleumier, P., 2005. How brains beware: neural mechanisms of emotional attention. Trends Cogn. Sci. 9 (12), 585–594.
Wittchen, H.-U., 2012. The Burden of Mood Disorders. American Association for the Advancement of Science, p. 15.
Wold, H., 1966. Estimation of principal components and related models by iterative least squares. In: Multivariate Analysis, pp. 391–420.
Wolff, A., Berberian, N., Golesorkhi, M., Gomez-Pilar, J., Zilio, F., Northoff, G., 2022. Intrinsic neural timescales: temporal integration and segregation. Trends Cogn. Sci. 26 (2), 159–173.
Yang, Y., Cui, Q., Lu, F., Pang, Y., Chen, Y., Tang, Q., et al., 2021. Default mode network subsystem alterations in bipolar disorder during major depressive episode. J. Affect. Disord. 281, 856–864.
Yang, C., Biswal, B., Cui, Q., Jing, X., Ao, Y., Wang, Y., 2024. Frequency-dependent alterations of global signal topography in patients with major depressive disorder. Psychol. Med. 54 (9), 2152–2161.
Yeo, B.T., Krienen, F.M., Sepulcre, J., Sabuncu, M.R., Lashkari, D., Hollinshead, M., et al., 2011a. The organization of the human cerebral cortex estimated by intrinsic functional connectivity. J. Neurophysiol. 106 (3), 1125–1165.
Yeo, B.T., Krienen, F.M., Sepulcre, J., Sabuncu, M.R., Lashkari, D., Hollinshead, M., et al., 2011b. The organization of the human cerebral cortex estimated by intrinsic functional connectivity. J. Neurophysiol. 1125–1165.
Yoshiike, T., Dallaspezia, S., Kuriyama, K., Yamada, N., Colombo, C., Benedetti, F., 2020. Association of circadian properties of temporal processing with rapid antidepressant response to wake and light therapy in bipolar disorder. J. Affect. Disord. 263, 72–79.
Zanto, T.P., Gazzaley, A., 2013. Fronto-parietal network: flexible hub of cognitive control. Trends Cogn. Sci. 17 (12), 602–603.
Zhang, J., Northoff, G., 2022. Beyond noise to function: reframing the global brain activity and its dynamic topography. Commun. Biol. 5 (1), 1350.
Zhang, L., Wu, H., Xu, J., Shang, J., 2018. Abnormal global functional connectivity patterns in medication-free major depressive disorder. Front. Neurosci. 12, 692.
Zhang, J., Magioncalda, P., Huang, Z., Tan, Z., Hu, X., Hu, Z., et al., 2019. Altered global signal topography and its different regional localization in motor cortex and hippocampus in mania and depression. Schizophr. Bull. 45 (4), 902–910.
Zhang, J., Tian, H., Li, J., Ji, S., Chen, S., Zhu, J., et al., 2020. Ketamine plus propofol-electroconvulsive therapy (ECT) transiently improves the antidepressant effects and the associated brain functional alterations in patients with propofol-ECT-resistant depression. Psychiatry Res. 287, 112907.
Zhang, Z., Zhang, H., Xie, C.-M., Zhang, M., Shi, Y., Song, R., et al., 2021. Task-related functional magnetic resonance imaging-based neuronavigation for the treatment of depression by individualized repetitive transcranial magnetic stimulation of the visual cortex. Sci. China Life Sci. 64, 96–106.
Zhang, Z., Zhang, Y., Wang, H., Lei, M., Jiang, Y., Xiong, D., et al., 2025. Resting-state network alterations in depression: a comprehensive meta-analysis of functional connectivity. Psychol. Med. 55, e63.
Zhou, Y., Wang, K., Liu, Y., Song, M., Song, S.W., Jiang, T., 2010. Spontaneous brain activity observed with functional magnetic resonance imaging as a potential biomarker in neuropsychiatric disorders. Cogn. Neurodyn. 4, 275–294.
Zhou, H.-X., Chen, X., Shen, Y.-Q., Li, L., Chen, N.-X., Zhu, Z.-C., et al., 2020. Rumination and the default mode network: meta-analysis of brain imaging studies and implications for depression. Neuroimage 206, 116287.
Zhu, W., Che, Y., Wang, Y., Jia, Z., Wan, T., Wen, J., et al., 2019. Study on neuropathological mechanisms of primary monosymptomatic nocturnal enuresis in children using cerebral resting-state functional magnetic resonance imaging. Sci. Rep. 9 (1), 19141.